On the Velocity Defect Law of Open Channel Flow

By

Yoshiaki IWASA* and Yoshio MURAMOTO*

(Received October 1962)

This paper describes the theoretical procedures for deriving a velocity defect law from the equations of motion and energy for turbulent mean flows in open channels, and the verification of the theoretical results from the experimental data of velocity distribution. Furthermore, by the use of the velocity defect law obtained and the boundary conditions imposed in the region near the wall, the velocity profile of turbulent mean flows in open channels and the mean velocity formula are presented.

1. Introduction

So far as the one-dimensional treatment in hydraulic analysis is concerned with the hydraulic behaviours of open channel flow, the steady-state hydraulics is solved by the method of singular point and that in an unsteady-state is also treated by the method of characteristics.

Many uncertainties, however, remain in the basic treatment of the classical one-dimensional hydraulic analysis and the modern hydraulic analysis for open channel flow combined with recent developments in modern hydrodynamics must be established to make further progress in the hydraulics of open channel flow. To make the foregoing intention possible, the entire staff of the Hydraulics Laboratory, Department of Civil Engineering, Kyoto University, joined together under the general supervision of Professor Tojiro Ishihara and an extensive research program for the establishment of modern hydraulic analysis for open channel flow was initiated.

The present study on the formulation of a velocity defect law for open channel flow in the light of recent knowledge of turbulence in modern hydrodynamics is one of the studies made as the first stage of the whole research program, with theoretical research on the hydrodynamic significance of the one-dimensional method in hydraulic analysis which will be seen in other publications[1),2)].

* Department of Civil Engineering

The velocity defect law is an empirical formula of the velocity profile for the turbulent mean flow, which was suggested by H. Darcy in 1858. Thereafter, L. Prandtl and T. von Kármán derived theoretically the functional form of the velocity defect law for pipe flow from some hypotheses in the turbulent velocity field. More recently, C. Millikan derived the logarithmic expression for the velocity distribution by means of a velocity defect law and the boundary conditions in the region near the wall, without referring to details of the turbulent structure. Thus, the velocity defect law is a universal formula for the time mean velocity distribution in a two-dimensional turbulent shear field, whereas that for open channel flow has not been discussed in detail and is mostly described by the following logarithmic expression,

$$\frac{\bar{u}_H-\bar{u}}{U_*}=-\frac{1}{\kappa}\ln\frac{z}{H}, \qquad (1)$$

in which $\bar{u}$: time-mean velocity at a distance z from bed, $\bar{u}_H$: surface velocity at $z=H$, U_* : shear velocity at channel bed, and κ : Kármán's universal constant.

Eq. (1) is, however, the resulting relation ignoring the influence of the force of gravity, namely, describing the motion of the lower layer dragged by the upper layer such as the behaviour of the turbulent boundary layer with no pressure gradient. For open channel flow under the predominant influence of the action of gravity, it is not adequate to derive the velocity defect law.

In connection with Eq. (1), J. Hinze[3)] introduced a new expression supplemented by a correction function of $h(z/H)+A$, and discussed the dynamic behaviour of the correction function from several experimental data.

As mentioned above, the logarithmic expression for the velocity profile, Eq. (1), is not suitable for open channel flow, and it would be necessary to reexamine the derivation of the velocity defect law for open channel flow and to verify experimentally the final equations obtained.

In this paper the velocity defect law for open channel flow is derived from the equations of motion and energy for turbulent mean flow in open channels, in consideration of velocity fluctuations, and the theoretical results obtained are examined by the experimental data of velocity distributions in smooth and rough channels. Furthermore, the velocity distribution and the mean velocity formula for open channel flow are derived from the velocity defect law by the use of the boundary conditions imposed in the region near the wall.

2. Derivation from Equation of Motion

Taking the x-axis along the channel bottom in the mean flow direction and the z-axis normal from the bottom, the two-dimensional uniform flow in open channels may be approximately expressed by

$$0 = \rho g \sin\theta + \frac{d}{dz}\left(\mu\frac{d\bar{u}}{dz} - \rho\overline{u'w'}\right), \tag{2}$$

$$0 = -\rho g \cos\theta - \frac{d\bar{p}}{dz} + \frac{d}{dz}(-\rho\overline{w'w'}), \tag{3}$$

in which, θ: constant inclination angle of channel bottom, $\bar{p}$: local mean pressure, g: acceleration of gravity, μ: dynamic viscosity, and $-\rho\overline{u'w'}$, $-\rho\overline{w'w'}$: Reynolds stresses.

The mean pressure distribution $\bar{p}$ is obtained by once integrating Eq. (3) with respect to z under the condition where $\bar{p}=0$ at $z=H$, which is

$$\bar{p} = \rho g \cos\theta(H-z) + \rho(\overline{w'w'}|_H - \overline{w'w'}|_z), \tag{4}$$

in which H is the depth of flow. Evidently in Eq. (4), $\bar{p}$ is the function of z and deviates from the hydro-static pressure distribution owing to the existence of the normal turbulent stress expressed in the second term of the right-hand side. The distributions of the normal turbulent stress $\rho\overline{w'w'}$ in Fig. 1 are the experimental data in the two-dimensional turbulent shear flow obtained by H. Reichardt[4]. As seen in Fig. 1, the value of $\overline{w'w'}$ increases rapidly for $z/H \leqq 0.2$, and becomes nearly constant for $z/H > 0.2$. Consequently, except in the small region near the boundary, $\bar{p}$ will be indicated by the hydrostatic pressure distribution even in the turbulent field.

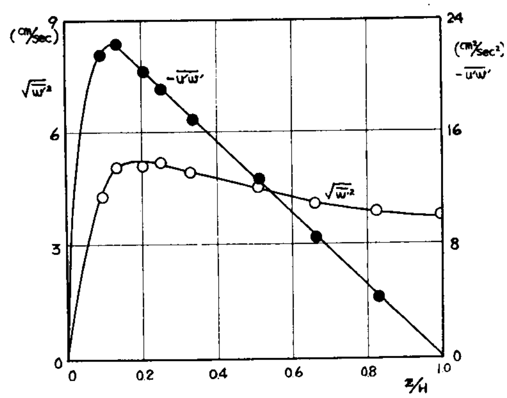

Fig. 1. Distribution of $-\overline{u'w'}$ and $\sqrt{\overline{w'^2}}$ (Exp. by Reichardt).

Ignoring the viscous term in Eq. (2), because the velocity defect law may be established in a fully developed turbulent field, and integrating Eq. (2) with respect to z, the turbulent shear stress finally becomes

$$-\rho\overline{u'w'} = \rho g \sin\theta(H-z), \tag{5}$$

under the condition of $-\rho\overline{u'w'}=0$ at $z=H$.

Namely, in the fully developed turbulent region the turbulent shear stress $-\rho\overline{u'w'}$ indicates a linear distribution. This fact will be also proved by Reichardt's experimental results in Fig. 1.

Considering the dynamic equilibrium between the gravity force and the tractive force in the uniform flow, the shear stress is expressed by

$$\tau_0 = \rho g H \sin\theta \,. \tag{6}$$

Applying the momentum-transfer theory by Prandtl or the similarity hypothesis of von Kármán to the turbulent shear stress $-\rho\overline{u'w'}$, Eq. (5) is rewritten as

$$-\rho\overline{u'w'} = \rho l^2 \left|\frac{d\bar{u}}{dz}\right| \frac{d\bar{u}}{dz} = \tau_0\left(1-\frac{z}{H}\right). \tag{7}$$

Now using Prandtl's and Kármán's hypotheses for the mixing length in Eq. (7), the velocity defect laws are derived as follows, respectively.

(i) Derivation from Prandtl's hypothesis: Putting $l=\kappa z$ in Eq. (7) and integrating with respect to z under the condition $\bar{u}=\bar{u}_H$ at $z=H$, the velocity defect law is obtained as

$$\frac{\bar{u}_H-\bar{u}}{U_*} = \frac{1}{\kappa}\left\{\ln\frac{(1+\sqrt{1-z/H})}{(1-\sqrt{1-z/H})} - 2\sqrt{1-\frac{z}{H}}\right\}. \tag{8}$$

(ii) Derivation from Kármán's hypothesis: Putting $l=\kappa\left(\frac{d\bar{u}}{dz}\right)\Big/\left(\frac{d^2\bar{u}}{dz^2}\right)$ in Eq. (7), and integrating twice with respect to z under the boundary conditions $\left.\frac{d\bar{u}}{dz}\right|_{z=\delta}=\infty$ at the lower margin of the fully developed turbulent region $z=\delta$ and $\bar{u}=\bar{u}_H$ at $z=H$ as above, the velocity defect law is expressed by

$$\frac{\bar{u}_H-\bar{u}}{U_*} = -\frac{1}{\kappa}\left\{\sqrt{1-\frac{z}{H}} + \ln\left(1-\sqrt{1-\frac{z}{H}}\right)\right\}. \tag{9}$$

Evidently, Eqs. (8) and (9) coincide with the expression in the velocity defect law of pipe flow with pressure gradient.

3. Derivation from Equation of Energy

The equation of energy for the turbulent motion in the two-dimensional steady flow may be written in the form

$$\begin{aligned}-\rho\overline{u'w'}\frac{d\bar{u}}{dz} = {} & \overline{\left(u'\frac{\partial}{\partial x}+w'\frac{\partial}{\partial z}\right)p'} + \frac{1}{2}\overline{\left(u'\frac{\partial}{\partial x}+w'\frac{\partial}{\partial z}\right)(u'^2+w'^2)} \\ & -\mu\frac{\partial}{\partial z}(\overline{u'e'_{xz}}+\overline{w'e'_{zx}}) + \frac{1}{2}\mu(\overline{e'^2_{xx}}+\overline{2e'^2_{xz}}+\overline{e'^2_{zz}}),\end{aligned} \tag{10}$$

in which

$$e'_{xx} = 2\frac{\partial u'}{\partial x}, \quad e'_{xz} = e'_{zx} = \left(\frac{\partial u'}{\partial z}+\frac{\partial w'}{\partial x}\right),$$

$$e'_{zz} = 2\frac{\partial w'}{\partial z}.$$

The left hand side represents the production of turbulence energy by the action of the shearing stress ($\bar{E}_{R'}$), the first term on the right hand side the convective diffusion of the turbulent pressure energy ($\bar{E}_{P'}$), the second term the convective diffusion of the turbulent kinetic energy ($\bar{E}_{F'}$), the third term the work done by the viscous shear stress ($\bar{E}_{V'}$), and the fourth term the energy dissipation into heat by the action of the viscosity ($\bar{E}_{D'}$). For the sake of simplicity in expression, Eq. (10) will be described with the symbols denoted above in brackets.

$$\bar{E}_{R'} = \bar{E}_{P'} + \bar{E}_{F'} + \bar{E}_{V'} + \bar{E}_{D'}. \tag{10$'$}$$

From the distribution of all the terms in Eq. (10)′ measured by Laufer[5] in pipe flow, the turbulent energy balance in any section of two dimensional turbulent shear flow is estimated as follows:

(i) wall-proximity region: $\bar{E}_{R'} \sim \bar{E}_{P'} + \bar{E}_{F'} + \bar{E}_{V'} + \bar{E}_{D'}$

(ii) intermediate region: $\bar{E}_{R'} \sim \bar{E}_{D'}$.

(iii) central or outer region: $\bar{E}_{F'} \sim \bar{E}_{D'}$.

The regions (i) and (iii) are, in general, much smaller than the region (ii), so that it may be considered that the production of turbulence energy ($\bar{E}_{R'}$) will be equal to the energy dissipation ($\bar{E}_{D'}$) in a large portion of the flow.

Now in order to derive the velocity defect law in the intermediate region, the characteristics of $\bar{E}_{R'}$ and $\bar{E}_D$ will be studied. Usually, the energy dissipation $\bar{E}_{D'}$ may be expressed by[6]

$$\bar{E}_{D'} \sim \rho \frac{(\sqrt{\overline{u'^2}})^3}{l}.$$

in which l is some representative length of the turbulent shear flow, such as mixing length, mean eddy size, etc. Furthermore, when the Reynolds number in the turbulent shear flow is high enough, $\sqrt{\overline{u'^2}}/U_*$ is represented, independently of the wall conditions, by a function of the relative flow depth z/H, as follows:

$$\frac{\sqrt{\overline{u'^2}}}{U_*} \sim f\left(\frac{z}{H}\right).$$

Using this relation, the energy dissipation may be expressed by

$$\bar{E}_{D'} = \rho U_*^3 f^3\left(\frac{z}{H}\right)\Big/ l. \tag{11}$$

On the other hand, the production of turbulence energy $\bar{E}_{R'}$ is expressed, using Eq. (7) in the previous section, by

$$\bar{E}_{R'} = -\rho\overline{u'w'}\frac{d\bar{u}}{dz} \sim \rho U_*^2\left(1-\frac{z}{H}\right)\frac{d\bar{u}}{dz}. \tag{12}$$

Consequently, in the intermediate region the following relation may be obtained from Eqs. (11) and (12),

$$l\frac{d\bar{u}}{dz} \sim U_* f^3\left(\frac{z}{H}\right)\Big/\left(1-\frac{z}{H}\right), \tag{13}$$

which is the basic relation of the velocity defect law in this region.

Now, assuming the expression of $\sqrt{\overline{u'^2}}/U_*$ by

$$\frac{\sqrt{\overline{u'^2}}}{U_*} \sim f\left(\frac{z}{H}\right) \sim \left(1-\frac{z}{H}\right)^n, \tag{14}$$

and $n=1/3$, Eq. (13) becomes

$$l\frac{d\bar{u}}{dz} \sim U_*.$$

This expression can be reduced to Eq. (1) by adopting either Prandtl's hypothesis or Kármán's hypothesis for the mixing length described in the previous section. Similarly, putting $n=1/2$, Eq. (13) becomes

$$l\frac{d\bar{u}}{dz} \sim U_*\Big/\sqrt{1-\frac{z}{H}},$$

which is also reduced to Eqs. (10) and (11) by the use of hypotheses of Prandtl and Kármán, respectively.

The experimental data of $\sqrt{\overline{u'^2}}/U_*$ measured by Laufer and Reichardt is shown in Fig. 2. From this figure it will be apparent that in the intermediate region ($\bar{E}_{R'} \sim \bar{E}_{D'}$) the distribution of $\sqrt{\overline{u'^2}}/U_*$ is consistent with the curve [Eq. (14)] for $n=1/2$ rather than that for $n=1/3$.

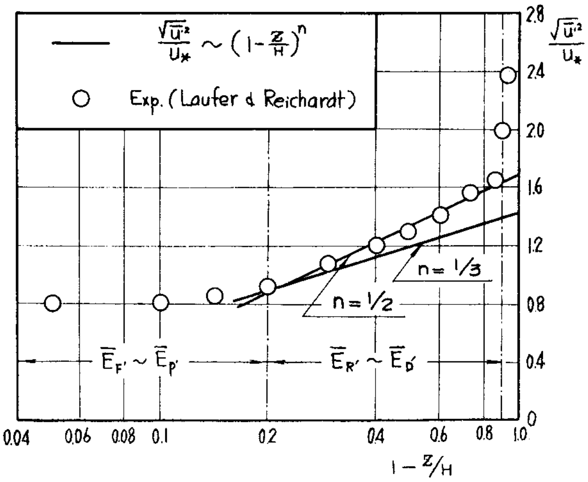

Fig. 2. $\frac{\sqrt{\overline{u'^2}}}{U_*}$ distribution and verification to n.

Consequently, as for the velocity defect law, it seems Eqs. (8) and (9) are more appropriate than Eq. (1) similar as with the result derived from the equation of motion in the previous section.

4. Experimental Verification

Now the three equations (1), (8), and (9) for the velocity defect law will be examined by the experimental results of the velocity distributions measured in open channels with smooth and rough walls.

The comparison between the theoretical curves and the experimental data measured in smooth channels of 0.01[7] and 0.002 slopes is shown in Figs. 3 and 4, respectively. In the case of $i=0.01$, evidently as seen in Fig. 3, the experimental data are plotted on the curves of Eqs. (8) and (9), and except the data under the flow condition of $Re=5.42\times10^2<2\times10^3$ (= the critical Reynolds number), agreed with the theoretical prediction described in the previous sections. However, in the case of $i=0.002$ (Fig. 4), a lesser agreement is shown; in the region of $0<z/H<0.5$ the experimental data are plotted nearly on the curves of Eqs. (8) and (9), but for $0.5<z/H\leqq1$ it is difficult to decide the dynamic predominance among the three theoretical curves. This results from the insufficient accuracy in experimental measurements and the three-dimensional influence due to the boundary shear not considered in the present study. Comparing the depth-width ratio (H/B) between the case of $i=0.01$ and that of $i=0.002$, $H/B=0.005\sim0.05$ in the former case whereas in the latter case $H/B=0.2\sim0.5$. Accordingly, the latter case will be more subject to the

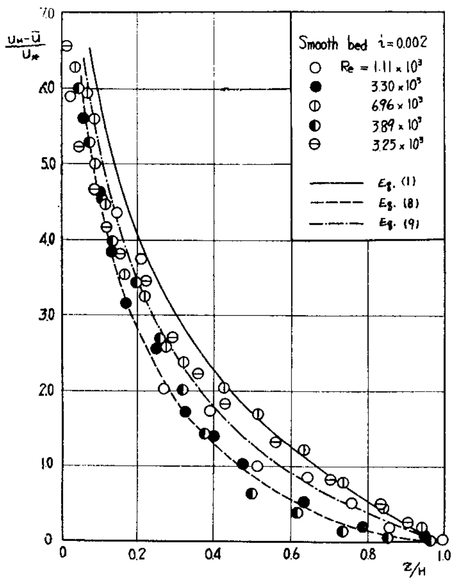

Fig. 3. Comparison between velocity defect law and experimental data (Exp. by Iwagaki)

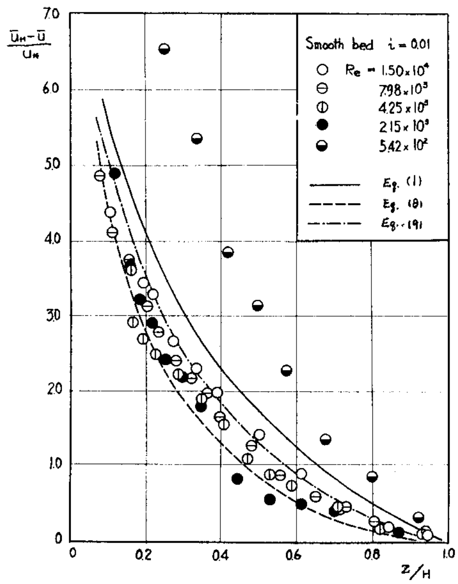

Fig. 4. Comparison between velocity defect law and experimental data (Exp. by Adachi and Muramoto)

influence of boundary shear.

The experimental results in rough channels[8] are shown in Figs. 5 and 6. All the experimental data, as seen in Fig. 5, are so scattered that the predominance among the three theoretical curves can not be discussed. But, as shown in Fig. 6, several data in this case indicate that in the smaller value of z/H the experimental data agree with the curve of Eq. (8) and approach the curve of Eq. (9) with the increase of the value z/H. It will be an interesting fact to consider that Prandtl's and Kármán's hypotheses are established in the region near the wall and the outer region, respectively.

As above mentioned, it is difficult to verify the theoretical results from the experimental data on the velocity distribution because of experimental inaccuracy and the influence of boundary shear. However, considering the procedures for deriving the velocity defect law described in sections 2 and 3, Eqs. (8) and (9) will be more rigorous than Eq. (1), though it is more difficult to decide the superiority between Eqs. (8) and (9). The difference between these two equations, as above, depends on the hypotheses of mixing length. In the main portion of flow section, Eq. (9) based on Kármán's hypothesis will be more adequate than Eq. (8) based on Prandtl's hypothesis. From a practical point of view as seen in Fig. 3~6, the curve of Eq. (9) will be suitable as the average value among three curves.

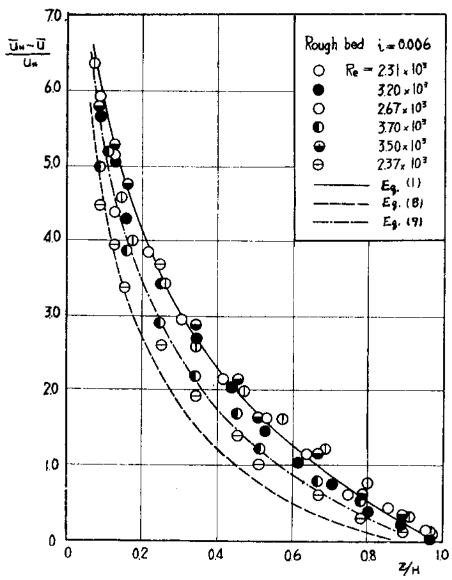

Fig. 5. Comparison between velocity defect law and experimental data (Exp. by Hosoi)

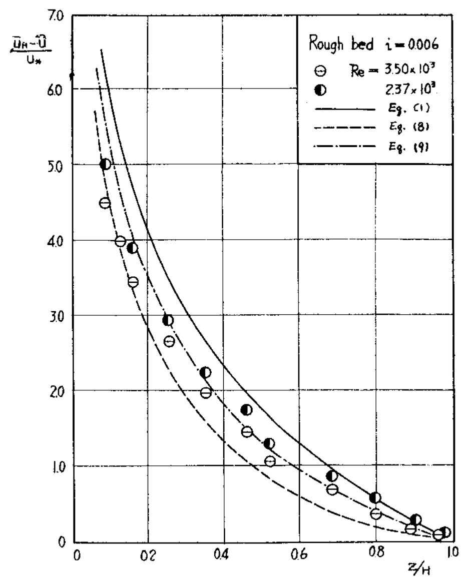

Fig. 6. Comparison between velocity defect law and experimental data (Exp. by Hosoi)

5. Velocity Distribution and Mean Velocity Formula

As described in the previous section, Eq. (9) is most suitable for the velocity defect law. Accordingly, in this section, the velocity distribution and the mean velocity formula will be derived from Eq. (9), in consideration of the boundary conditions imposed at the channel bed.

5-1. Velocity Distribution

When the boundary condition near the wall: $\bar{u}=\bar{u}_\delta$ at $z=\delta$ is applied, instead of using the free surface condition in section 2; $\bar{u}=\bar{u}_H$ at $z=H$, the velocity distribution is obtained as follows:

$$\frac{\bar{u}}{U_*}=\frac{1}{\kappa}\left[\sqrt{1-\frac{z}{H}}+\ln\left(1-\sqrt{1-\frac{z}{H}}\right)\right]-\frac{1}{\kappa}\left[\sqrt{1-\delta_0}+\ln\left(1-\sqrt{1-\delta_0}\right)\right]+\frac{\bar{u}_\delta}{U_*} \tag{15}$$

in which $\delta_0=\delta/H$. In general, it is assumed $\delta\ll H$, that is, $\delta_0\ll 1$ under the turbulent open channel flow condition. Developing the second term on the right in Eq. (15) with respect to δ_0 in a series, and ignoring the second and higher terms of δ_0 in order, Eq. (15) becomes

$$\frac{\bar{u}}{U_*}=\frac{1}{\kappa}\left\{\sqrt{1-\frac{z}{H}}+\ln\left(1-\sqrt{1-\frac{z}{H}}\right)\right\}-\frac{1}{\kappa}\left(1-\frac{1}{2}\delta_0-\ln\frac{\delta_0}{2}\right)+\frac{\bar{u}_\delta}{U_*}. \tag{16}$$

On the other hand, $\bar{u}_\delta/U_*$, is shown as follows, by considering the connection between the turbulent zone and the laminar sublayer,

$$\frac{\bar{u}}{U_*}=\frac{U_*\delta}{\nu}=\delta_0 Re^*$$

in which $Re^*=U_*H/\nu$. Furthermore, from the dimensional consideration in analysis for the laminar sublayer it may be expressed as $\delta\sim\nu/U_*$, namely,

$$\delta_0=\alpha\frac{1}{Re^*}. \quad (\alpha=\text{proportional constant})$$

Inserting the above expressions into Eq. (16) and putting Kármán's constant $\kappa=0.4$, the final form of velocity distribution is obtained as follows:

$$\left.\begin{aligned}\frac{\bar{u}}{U_*}&=2.5\left\{\sqrt{1-\frac{z}{H}}+\ln\left(1-\sqrt{1-\frac{z}{H}}\right)\right\}\\&\quad+a_s+\varphi_s(Re^*)\\ \text{where}\qquad&\\ a_s&=\alpha-5.75\log\alpha-0.772\\ \varphi_s(Re^*)&=1.25\frac{\alpha}{Re^*}+5.75\log Re^*\end{aligned}\right\} \tag{17}$$

Consequently, when U_*, H, and Re^* are given in the flow considered, the velocity distribution in a turbulent region of open channel flow is determined by Eq. (17). The proportional constant a, as seen in Fig. 7, tends to take a constant value. But, further experimental verification is still necessary to determine a.

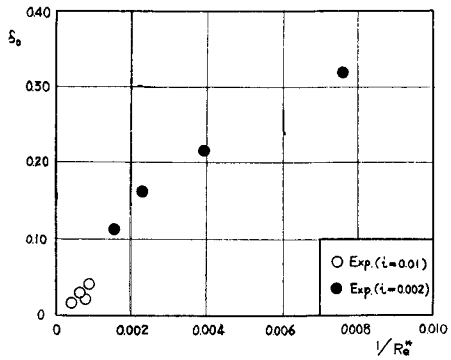

Fig. 7. Relations between δ_0 and 1/Re*.

5-2. Mean Velocity Formula

Integrating the velocity distribution over the whole region involving the laminar sublayer and the turbulent zone, the mean velocity formula is obtained as follows:

$$\left.\begin{aligned}\frac{U_m}{U_*} &= \frac{1}{H}\left[\int_0^\delta \frac{U_* z}{\nu}dz + \frac{1}{\kappa}\int_\delta^H \left\{\sqrt{1-\frac{z}{H}} + \ln\left(1-\sqrt{1-\frac{z}{H}}\right)\right.\right.\\ &\quad \left.\left. -\sqrt{1-\delta_0} - \ln\left(1-\sqrt{1-\delta_0}\right) + \kappa\frac{\bar{u}_\delta}{U_*}\right\}dz\right]\\ &= \delta_0\left(\frac{3}{2}-\delta_0\right)Re^* - \frac{1}{\kappa}\left\{\frac{1}{3}(1-\delta_0)^{3/2} + \frac{1}{2}(1-\delta_0)\right.\\ &\quad \left. + (1-\delta_0)^{1/2} + \ln\left(1-\sqrt{1-\delta_0}\right)\right\}.\end{aligned}\right\} \tag{18}$$

Further applying the same approximation as indicated in the previous article (5-1) to this case, and putting $\delta_0 = a/Re^*$ and $\kappa=0.4$ in Eq. (18), the mean velocity formula is expressed by

$$\left.\begin{aligned}\frac{U_m}{U_*} &= A_s + \Phi_s(Re^*)\\ \text{where}\quad A_s &= 1.5\,a - 5.75\log a - 2.85\\ \Phi_s(Re^*) &= \frac{a}{Re^*}(3.75-a) + 5.75\log Re^*.\end{aligned}\right\} \tag{19}$$

Although the above description concerns only the velocity formula in a smooth channel, the formula in a rough channel may be obtained by similar procedure under the condition where $\delta = \beta k$ (β: a proportional constant, k: the representative length of roughness).

6. Conclusion

Determining the universal function of the velocity distribution in connection with the investigation of frictional resistance, diffusion phenomena etc.

in open channel flow is still an important basic problem.

In this paper, the theoretical procedures for deriving a velocity defect law, the so-called universal function of velocity distribution in two-dimensional turbulent shear flow, is discussed, and the experimental verification of the theoretical results is also made. Furthermore, in connection with practical use, the velocity distribution and the mean velocity formula for open channel flow are derived by means of the velocity defect law and the wall conditions.

However, in order to verify the theoretical results obtained in the present study in detail, further experimental research is needed.

Acknowledgment

The authors would like to express their sincere appreciation to Professor Ishihara for his comments and consultation during the course of the present work, and many thanks are due to Mr. H. Imamoto for his assistance in calculations.

References

1) Iwasa, Y.; Paper in Seminary b, 9th Convention of IAHR, Dubrovnik, Yugoslavia, 1961.
2) Ishihara, T. and Iwasa, Y.; Proc. 1st Conference on Hydraulics and Fluid Mechanics, Univ. of Western Australia, Nedland, Australia, 1962.
3) Hinze, J. O.; "Turbulence", McGraw-Hill, 1959.
4) Reichardt, H.; ZAMM, Band **18**, 358, 1939.
5) Laufer, J.; NACA report 1174, 1954.
6) Goldstein, S.; "Modern Developments in Fluid Dynamics", Vol. 1, Oxford, 1938.
7) Iwagaki, Y.; Doctoral Thesis, 1955.
8) Hosoi, M.; Research of Civil Eng., 1945.